

# Calcium-Induced Voltage Gating in Single Conical Nanopores

Zuzanna S. Siwy,<sup>\*,†</sup> Matthew R. Powell,<sup>\*,†</sup> Alexander Petrov,<sup>†</sup> Eric Kalman,<sup>†</sup> Christina Trautmann,<sup>‡</sup> and Robert S. Eisenberg<sup>§</sup>

*Department of Physics and Astronomy, University of California, Irvine, Irvine, California 92697, Gesellschaft fuer Schwerionenforschung, Planckstrasse 1, 64291 Darmstadt, Germany, and Department of Molecular Biophysics & Physiology, Rush Medical College, Chicago, Illinois 60612*

Received May 16, 2006; Revised Manuscript Received June 19, 2006

## ABSTRACT

We examine time signals of ion current through single conically shaped nanopores in the presence of sub-millimolar concentrations of calcium ions. We show that calcium induces voltage-dependent ion current fluctuations in time in addition to the previously reported negative incremental resistance (*Nano Lett.* 2006, 6, 473–477). These current fluctuations occur on the millisecond time scale at voltages at which the effect of negative incremental resistance was observed. We explain the fluctuations as results of transient binding of calcium ions to carboxyl groups on the pore walls that cause transient changes in electric potential inside a conical nanopore. We support this explanation by recordings of ion current in the presence of manganese ions that bind to carboxyl groups 3 orders of magnitude more tightly than calcium ions. The system of a single conical nanopore with calcium ions is compared to a semiconductor device of a unijunction transistor in electronic circuits. A unijunction transistor also exhibits negative incremental resistance and current instabilities.

**Introduction.** Interest in nanopores has been stimulated by discoveries of the importance of biological channels in many physiological processes of a living organism<sup>1,2</sup> as well as the application of channels in building single molecule sensors.<sup>3</sup> Transport properties of nanopores are very different from transport properties of micrometer size pores. Transport through nanopores is modulated strongly by interactions with the walls of the pore, because nanopores are so small that transported ions cannot easily avoid the walls, particularly their electric fields. We have shown previously that electrical interaction of potassium ions with negative permanent surface charge in conically shaped nanopores makes these pores cation selective and rectifies the ion current that passes through these pores.<sup>4</sup> Potassium ions flow more easily from the narrow entrance toward the wide opening of the conical nanopores.<sup>5–8</sup>

In a recent Letter<sup>9</sup> we studied transport effects induced by electrostatic interactions together with chemical binding of ions inside a conical nanopore. We studied single conical nanopores in the presence of calcium ions that could transiently bind to the walls of the pores, thus transiently changing the internal electric potential of the nanopores. These interactions produced a negative incremental resistance observed in current–voltage curves as a decrease in the

magnitude of ion current with an increase in the magnitude of applied voltage. In this Letter we show that transient binding of calcium ions also induces voltage-dependent fluctuations of ion current through single conical nanopores. We discuss similarities of our system of a single conical nanopore with calcium to a semiconductor device, the unijunction transistor.<sup>10,11</sup> A unijunction transistor also exhibits negative incremental resistance and current instabilities. This semiconductor device regulates electron current, while our device controls movement of ions in a water solution. The relation between negative incremental resistance and ion current instabilities is discussed here as well.

**Experimental Section. (A) Materials.** The nanopores studied in this Letter were prepared in 12  $\mu\text{m}$  thick foils of polyethylene terephthalate (PET) (Hostaphan RN12, Hoechst). Three centimeter diameter disks of these foils were irradiated with single heavy ions at the linear accelerator (UNILAC) at the Gesellschaft fuer Schwerionenforschung, Darmstadt, Germany.<sup>12,13</sup> Chemical etching of these single ion irradiated foils leads to formation of single pores. Conically shaped nanopores were prepared by etching the foils from one side with 9 M NaOH as described in refs 5 and 6, forming tapered-cone nanopores with two openings, one with diameter  $\sim 1 \mu\text{m}$  and the other with diameter  $\sim 2 \text{ nm}$ . The wide opening of the pore is the base (with diameter  $d_b$ ); the narrow opening of the pore is the tip with diameter  $d_t$ . Etching of PET with NaOH hydrolyzes ester bonds of PET and produces carboxylate groups with surface charge density of carboxylate groups estimated to be  $\sim 1.5 \text{ e/nm}^2$ .<sup>14,15</sup>

\* Corresponding authors. E-mail: zsiwy@uci.edu (Z.S.S.), mrpowell@uci.edu (M.R.P.).

<sup>†</sup> University of California.

<sup>‡</sup> Gesellschaft fuer Schwerionenforschung.

<sup>§</sup> Rush Medical College.

**(B) Ion Current Recordings.** Ion currents were measured in a conductivity cell<sup>5,6</sup> with Ag/AgCl electrodes (Bioanalytical Systems Inc., West Lafayette, IN) and recorded with the amplifier Axopatch 200 B (Molecular Devices Inc.) in voltage-clamp mode using a low pass Bessel filter of 2 kHz. The signal was digitized with Digidata 1322 A (Molecular Devices Inc.) at 10 kHz, and viewed with Clampex 9.2. We typically recorded 2 min long time series with 50 mV steps of potential. The potential differences are computed as  $V_b - V_t$  where  $V_b$  and  $V_t$  are potentials of the electrodes on the base and tip side, respectively. Ohm's law is then written as  $i = g(V_b - V_t)$  with  $g \geq 0$  and thus positive  $i$  means that cations flow from base to tip. As shown previously, PET nanopores at neutral and basic pH are cation selective.<sup>4,16</sup> The cations flow with less resistance from the tip toward the base than from base to tip.

**Results and Discussion.** We recorded ion current at 0.1 M KCl, pH 8, before adding calcium and after adding calcium at concentrations between 0.1 and 1.0 mM  $\text{CaCl}_2$ . Since the concentration of potassium ions is much higher than concentration of calcium ions, we neglect the current carried by calcium ions themselves and treat calcium ions just as a modulator of potassium ion flow and not the main current carrier.<sup>17</sup>

Figure 1 shows examples of ion current time series recorded at 0.1 M KCl and 0.3 mM  $\text{CaCl}_2$  at pH 8 for a pore with  $d_t = 4$  nm and  $d_b = 1.5$   $\mu\text{m}$ . Before calcium is added, the signals of ion current are very stable with a narrow distribution of current values (Figure 1).

After calcium is added, the character of the ion current changes dramatically and becomes clearly voltage-dependent. For  $V_b - V_t > 0$ , and also for small magnitudes of negative  $V_b - V_t$ , the ion current signals remain "quiet" and currents with calcium are comparable to currents recorded without calcium. For  $V_b - V_t < -300$  mV, calcium induced very strong fluctuations of ion current with amplitudes reaching 100% value of the current signal. For  $V_b - V_t < -600$  mV, histograms of ion currents suggest existence of two states in ion current values. We call the low level of ion current a closed state of the pore and the level with higher current we call an open state of the nanopore using the language of biophysics. Note that the current fluctuations are hundreds of picoamps in magnitude. Calcium reduced the current recorded for  $V_b - V_t < -300$  mV compared to the currents recorded before adding calcium (Figure 1). For example, the average value of ion current at  $-500$  mV and 0.1 M KCl is  $-800$  pA. After 0.3 mM  $\text{CaCl}_2$  is added, the average current at  $-500$  mV dropped to  $-74$  pA.

Figure 2 shows a current–voltage curve reconstructed from current–time series. The signals were averaged over the whole 2 min duration of the recordings, and mean values and standard deviations were calculated. For  $V_b - V_t < -300$  mV, larger magnitudes of voltages induced smaller magnitudes of ion current, an effect called negative incremental resistance that we reported before.<sup>9</sup> Subsequent recording of time series of ion current gives us additional information about the time scale of this effect not available in the original experiments. For 0.3 mM  $\text{CaCl}_2$ , at  $-300$  mV where the

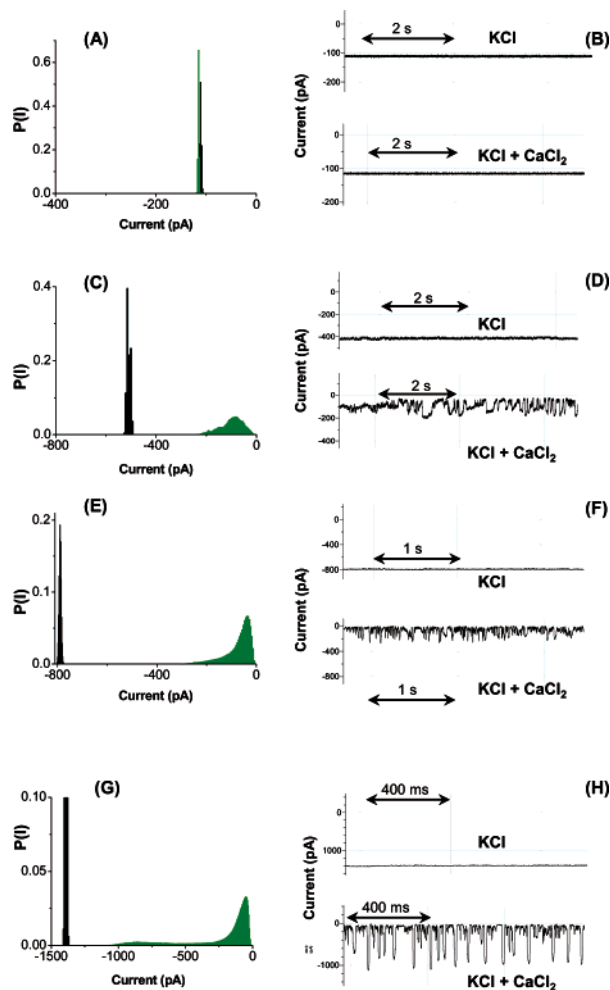


**Figure 1.** Ion current time series through a single conically shape nanopore at PET with  $d_t = 4$  nm. Frequency histograms of ion current  $P(I)$  recorded at  $-50$  mV (A),  $-350$  mV (C),  $-500$  mV (E), and  $-900$  mV (G): in black for 0.1 M KCl and in green for 0.1 M KCl and 0.3 mM  $\text{CaCl}_2$ , pH 8. B, D, F, and H fragments of ion current recordings before and after adding calcium at  $-50$  mV (B),  $-350$  mV (D),  $-500$  mV (F), and  $-900$  mV (H). Voltage is defined as  $V_b - V_t$ .

negative incremental resistance starts, the current starts to decrease very slowly: during 2 min of recordings at  $-300$  mV the current magnitude decreased from  $-450$  to  $-380$  pA. We also show a fragment of signal at  $-350$  mV that was recorded immediately after the voltage was switched from its previous value of  $-300$  mV (that had been maintained for 2 min). Negative incremental resistance and instabilities in ion current signals occur at the same time, as far as we can tell.

Similar measurements were performed with larger concentrations of  $\text{CaCl}_2$ . For larger calcium concentrations, the effect of negative incremental resistance occurred more abruptly (Figure 2B) and appeared at voltages of a smaller magnitude. Negative incremental resistance and instabilities in ion current signals again occurred at the same time.

We studied the time scale of ion current fluctuations where the current shows a distinct two-state behavior, in the region of  $-800 < V_b - V_t < -1000$  mV for 0.3 mM  $\text{CaCl}_2$ . Figure 3 shows a fragment of ion current time series together with

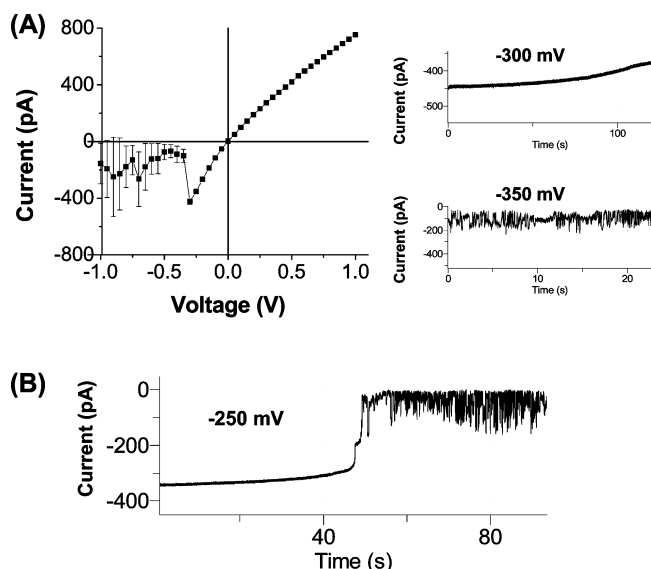


**Figure 2.** (A) Current–voltage curve obtained by averaging 2 min recordings of ion current through a single conically shaped nanopore at PET with the tip opening of 4 nm. The recordings were performed at 0.1 M KCl with 0.3 mM CaCl<sub>2</sub> every 50 mV. As insets, fragments of ion current recorded at –300 and –350 mV are shown. Voltage is defined as  $V_b - V_t$ . (B) Ion current recording at 0.1 M KCl, 0.7 mM CaCl<sub>2</sub>, pH 8,  $V_b - V_t = -250$  mV.

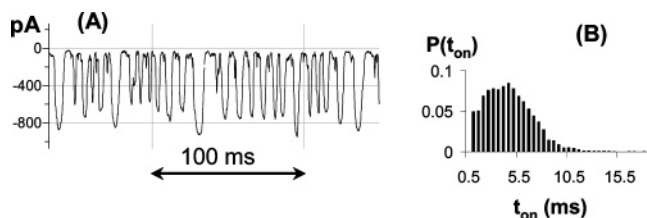


**Figure 3.** Fragment of ion current signal (A) through a single PET nanopore with  $d_t = 4$  nm recorded at 0.1 M KCl, 0.3 mM CaCl<sub>2</sub>, pH 8,  $V_b - V_t = -950$  mV, together with a histogram of durations of the open state  $t_{on}$  (B).

a histogram of the duration of open states for  $V_b - V_t = -950$  mV. The data suggest that the duration histogram is not uniform: some durations of the open state are more probable than others. Figure 4 shows examples of ion current recordings performed for various calcium concentrations at  $V_b - V_t = -950$  mV. As we can see, there is an optimal range for formation of the discrete fluctuations of ion current, namely, between 0.2 mM CaCl<sub>2</sub> and 0.7 mM CaCl<sub>2</sub>. For this nanopore, at 0.1 mM CaCl<sub>2</sub>, the open events occur in bursts, while for very high calcium concentrations such as 1.0 mM CaCl<sub>2</sub>, the pore is blocked.

**(A) Effect of Calcium on Electrochemical Potential of a Conical Nanopore.** To explain the effect of ion current fluctuations in the presence of calcium, we considered the profile of electric potential of an ion inside a conical nanopore with permanent surface charges. Two independent approaches for modeling of this potential profile indicated that the profile has an asymmetric shape, visualized for simplicity as a piecewise linear ratchet tooth.<sup>6,7,18</sup> We assume that calcium ions stay near the COO<sup>−</sup> groups at the pore walls—within a Debye length to be precise—for times comparable to the time that potassium ions need to trans-

locate the pore.<sup>9</sup> We think that calcium ions remain near the pore walls (i.e., are “bound” there), because the density of carboxylate groups is very high, comparable to the density of COOH groups in ethylenediaminetetraacetic acid (EDTA). One can view the binding as a result of the crowded charge mechanism<sup>19–24</sup> or one can take the more traditional chemical view that COO<sup>−</sup> groups form “coordination bonds” with Ca<sup>2+</sup>.<sup>25</sup> In this latter (somewhat vague but appealing) view, COO<sup>−</sup> groups are donors of an electron pair to the metal ions: metal ions function therefore as Lewis acids while COO<sup>−</sup> groups act as Lewis bases.<sup>25</sup> What is important for our discussion here is that calcium binds to the four carboxylate groups of EDTA with effective binding (formation) constants  $K_{eff}$  as high as  $10^8$  M<sup>−1</sup>.<sup>19,26</sup> What is also crucial is that EDTA chelates various divalent cations with different  $K_{eff}$ , dependent on size and chemical properties of the mobile ions and the EDTA.<sup>25</sup> It is important to remember that  $K_{eff}$  is a function of the concentration of most ions, i.e., ionic strength, local electrical potential, as well as position, in many situations, despite the name binding “constant”.

To support the idea of binding of divalent cations to carboxylate groups, we also performed ion current measurements in the presence of manganese ions (Figure 5A).  $K_{eff}$  of EDTA for Mn<sup>2+</sup> ions is 3 orders of magnitude larger than that for calcium ions.<sup>26</sup> We imagine that manganese ions bind stronger to carboxylate groups in the nanopore. Therefore the pore stays predominantly in the closed state in the presence of Mn<sup>2+</sup>, opening much less frequently than in the presence of calcium ions (compare Figure 5B with Figure 1G).

**(B) Similarities between Conical Nanopores with Calcium and Semiconductor Unijunction Transistors.** The electrical signals that we observed with conical nanopores in the presence of calcium—namely, negative incremental resistance and current fluctuations—are observed in circuits containing semiconductor devices such as unijunction transistors.<sup>10,11</sup> Unijunction transistors typically consist of n type semiconductor material into which p type semiconductor material is diffused to make the emitter. No current flows between the emitter and the base until a voltage is applied between them. When the voltage of the emitter is increased to some threshold value, the diode is forward biased and a flow of ion current is observed. If the circuit contains a capacitor as shown in Figure 6A, the capacitor is charged through resistor  $R_{ch}$ . When the voltage at the capacitor reaches a threshold value, current flows between emitter and base 1, discharging the capacitor. The cycle is repeated, making relaxation oscillations. Relaxation oscillations have a characteristic shape due to exponential charging of the capacitor, observed as an exponential increase of voltage at the emitter with time constant equal to the product of  $R_{ch}$  and capacitor  $C$ .

We think that our conical nanopores—with permanent surface charges and calcium binding to carboxylate groups—operate rather like a unijunction transistor as we now describe qualitatively, while we await a quantitative theory. The tip of our conical nanopore, where the electric potential has its minimum, is called “base 1”; the rest of the pore is base 2

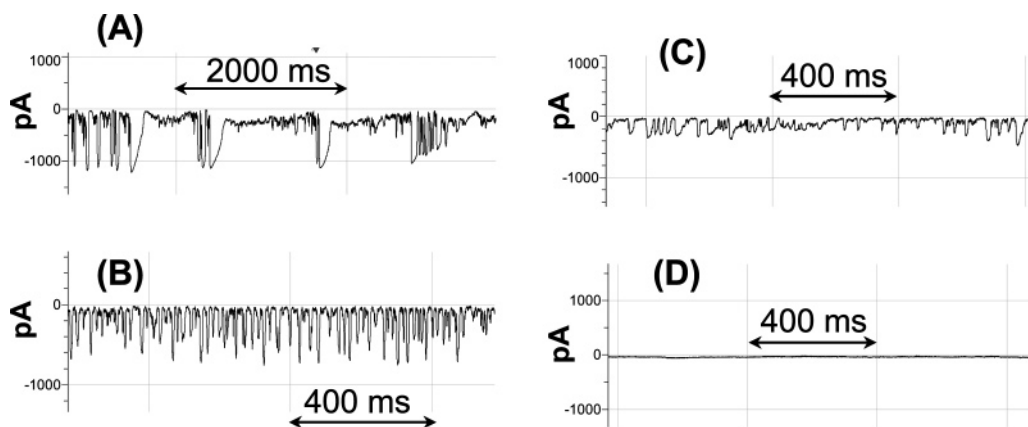


**Figure 4.** Fragments of ion current recorded at 0.1 M KCl, pH 8, for  $V_b - V_t = -950$  mV, with 0.1 mM  $\text{CaCl}_2$  (A), 0.3 mM  $\text{CaCl}_2$  (B), 0.7 mM  $\text{CaCl}_2$  (C), and 1.0 mM  $\text{CaCl}_2$  (D). Data in Figures 1–4 were recorded for the same PET nanopore with  $d_t = 4$  nm and  $d_b = 1500$  nm.

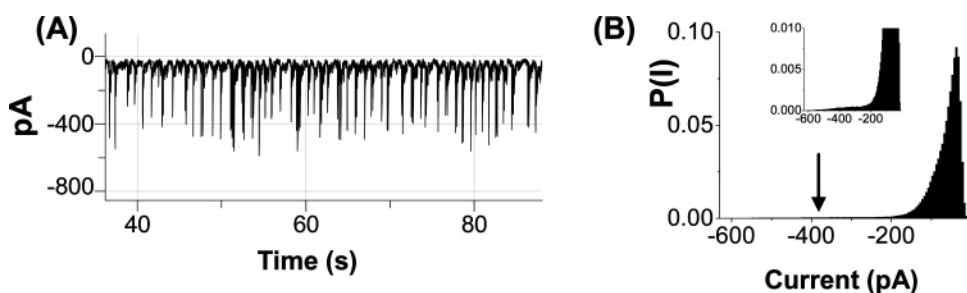


**Figure 5.** Fragments of ion current recorded at 0.1 M KCl, pH 8 for  $V_b - V_t = -950$  mV, with 0.1 mM  $\text{MnCl}_2$  (A) together with frequency histogram  $P(I)$  of ion current values (B). The inset shows details of the histogram for open states. Diameter of the tip opening  $d_t$  of this PET nanopore was 6 nm.

(Figure 6B). The pore walls at the tip where calcium can bind are our emitter. Without calcium, for  $V_b - V_t < 0$  our diode is biased in the forward direction, because the total potential, originating from internal charges and induced by current flow, does not contain a deep cation trap.<sup>4,6–8</sup> When  $V_b - V_t > 0$ , we suppose that the electric potential does have a deep cation trap.<sup>4,8</sup> For negative values of  $V_b - V_t$  we therefore observe large currents. When we add calcium to the system, calcium diffuses to the pore and accumulates close to the tip of the pore, where the net potential originating from internal charges and induced by current flow has the smallest magnitude. Without voltage applied, the number of calcium ions at the tip is however not enough to change the resistance of the pore in a significant way. When values of  $V_b - V_t$  become more negative, the number of calcium ions arriving at the tip of the pore increases, so does the number of calcium ions at the tip of the pore. We think that the accumulation of calcium ions changes the overall potential profile rather as it changes the potential profile in the ratchet mechanisms,<sup>27</sup> so the overall current decreases in magnitude although the voltage  $V_b - V_t$  (applied across the membrane) increases in magnitude. For 0.3 mM  $\text{CaCl}_2$  this decrease of ion current occurred for potentials less than  $|V_b - V_t| \approx -500$  mV. It is important to note that the binding of calcium to the  $\text{COO}^-$  groups, described by  $K_{\text{eff}}$ , depends on the potential within the channel, which in turn depends both on the applied potential  $V_b - V_t$  and on all other charged groups in the pore. The interdependence of potential, finite diameter, charge, and

binding is an essential feature of the crowded charge models of selectivity.<sup>19–23</sup>

Figure 6C shows the piecewise linear distribution of internal electric potential with the potential well equal to  $-200$  mV as shown in ref 28. We assume that the potential well is located 5 nm from the tip of the pore and that the internal potential decays over the first 125 nm, where 80% of the pore resistance is focused. The dotted line shows how the external voltage  $V_b - V_t = -500$  mV is distributed along the first 125 nm of the pore when we take into account only the geometry of the pore.<sup>28</sup> The dotted-dashed line presents the “total potential” as the sum of these two potentials, showing a shallow cation trap at the tip of the pore. A complete solution of Poisson’s equation and the crowded charge model is needed to make a more realistic computation of the total potential, but such a calculation is unfortunately not feasible at this time. Locally, at the tip between  $\sim 50$  and 100 nm (Figure 6C) the local electric force (defined as gradient of the potential) acting on calcium and potassium ions has smaller magnitude than that in other parts of the pore.

This is a coupled system because calcium binding to the pore walls changes the profile of internal potential together with the net potential acting on calcium and potassium ions. With calcium bound to the pore surface, the total potential is closer to the situation without any internal potential, where no trap or flattening of the potential occurs. We think that threshold occurs at a combination of values of  $V_b - V_t$  and

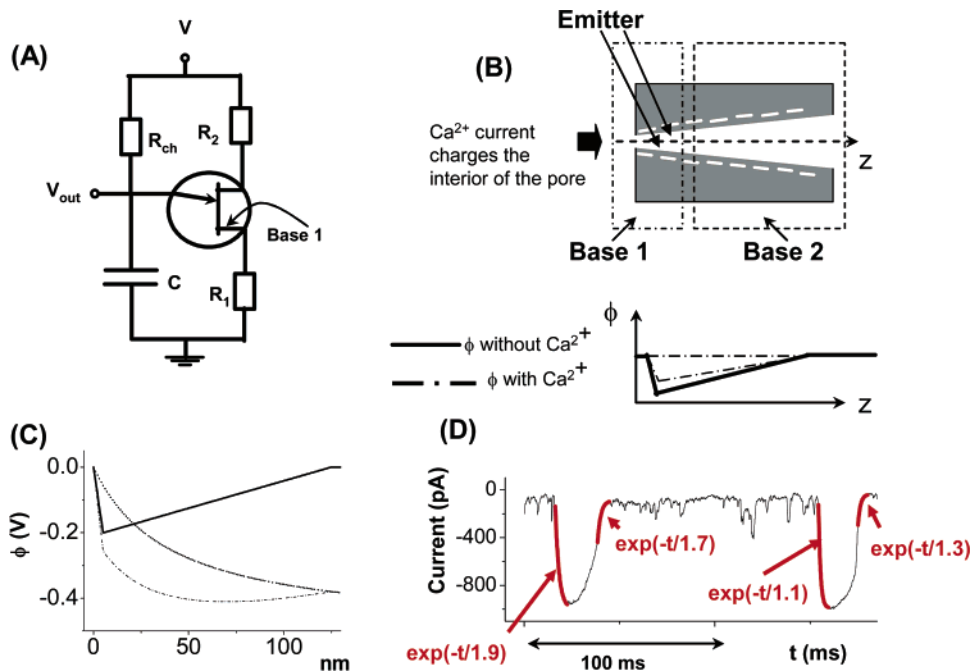


**Figure 6.** (A) Electric circuit with unijunction transistor that produces relaxation oscillations. (B) Schematic representation of a conical nanopore with negative surface charges on the pore walls together with the shape of electric potential before adding calcium (continuous line) and possible distributions of the potential after adding calcium (dashed lines). (C) (solid line) Simplified, piecewise linear representation of internal potential originating from surface charges of a conical nanopore with  $V_b - V_i = 0$ .<sup>6,7,28</sup> (dotted line) Distribution of  $V_b - V_i = -500$  mV inside a conical nanopore with  $d_t = 4$  nm and  $d_b = 1500$  nm. The dashed-dotted line presents the sum of internal and external ( $V_b - V_i$ ) potentials over the length of 125 nm from the tip. (D) Fragment of recording shown in Figure 1H with two open events fitted with a function  $y = A \exp(-t/\tau) + y_0$ . The exponents with values of  $\tau$  are given in the figure.

of the number of calcium bound to the pore. At the threshold, the net electric force acting on calcium ions is high enough to bring the value of  $K_{eff}$  (which is not a constant despite its name) to the level that ensures dwell times of calcium in the pore comparable or shorter to the translocation time of potassium ions. This threshold would explain the burst of open current, indicating collective exit of calcium ions. The internal potential goes back to its previous level, and the net electric force acting on calcium decreases. Calcium can therefore bind to the pore walls again, changing gradually the local net force acting on ions, and the cycle repeats again.

The exponential shape of the majority of open states in current fluctuations (Figure 6D) also suggests charging/discharging of the capacitor, providing additional evidence for relaxation character of observed current fluctuations with millisecond time scale fluctuations.

The previous paragraph describes one explanation of our findings, but others are undoubtedly possible. There are many other effects that can occur, and a quantitative analysis is needed although difficult. For example, we did not take into account mutual repulsion of calcium ions that might also contribute to increase of the potential.<sup>15</sup> Achieving the threshold potential at which the dwell time of calcium becomes shorter than the translocation time of potassium ions would correspond to the threshold voltage at the emitter of an unijunction transistor that induces flow of current between emitter and base 1. A quantitative model is needed to describe this important effect precisely.

In our previous paper, we discussed the effect of negative incremental resistance in light of the flashing ratchet

concept.<sup>9</sup> We suggested a model in which calcium ions binding to the  $COO^-$  groups would change the potential profile from a ratchet tooth shape to the flat shape. This change of shape pumps the potassium ions in the opposite direction to the applied electric field. It is possible that the binding mechanism shown here could produce a flashing ratchet. A convincing model must include crowded charge effects, spatial and time dependence of potential, voltage dependence of ionization of  $COO^-$  groups,<sup>29</sup> as well as fluctuations of surface charge of PET pores<sup>15</sup> and charge-charge interactions on the time scale of the current fluctuations, usually milliseconds. This millisecond time scale is inaccessible to molecular dynamics and present models of crowded charge do not describe spatial dependence very well or time dependence at all.

**Conclusions.** We describe a system with single conically shaped nanopores that produces voltage-dependent ion current fluctuations in the presence of sub-millimolar concentrations of calcium ions. These current instabilities are described as relaxation fluctuations due to binding and unbinding of calcium ions to carboxylate groups, which produce charging and discharging of the capacitor element of our nanopore system and thus change the electrical potential. The transport properties of our system were compared to unijunction transistor. In our future efforts, we will try to describe the effect quantitatively.

**Acknowledgment.** Irradiation with swift heavy ions was performed at the Gesellschaft fuer Schwerionenforschung

(GSI), Darmstadt, Germany. We are very grateful for discussions with Professor Charles R. Martin and Professor Clare Yu. The work of R.S.E. was supported in part by NIH grant GM076013.

## References

- (1) Hille, B. *Ionic Channels of Excitable Membranes*, 2nd ed.; Sinauer: Sunderland, MA, 1992.
- (2) Ashcroft, F. M. *Ion Channels and Disease*; Academic Press: New York, 1999.
- (3) Bayley, H.; Martin, C. R. *Chem. Rev.* **2000**, *100*, 2575–2594.
- (4) Siwy, Z. *Adv. Funct. Mater.* **2006**, *16*, 735–746.
- (5) Apel, A.; Korchev, Y. E.; Siwy, Z.; Spohr, R.; Yoshida, M. *Nucl. Instrum. Methods Phys. Res., Sect. B* **2001**, *184*, 337–346.
- (6) Siwy, Z.; Fulinski, A. *Phys. Rev. Lett.* **2002**, *89*, 198103/1–198103/4.
- (7) Siwy, Z.; Fulinski, A. *Am. J. Phys.* **2004**, *72*, 567–574.
- (8) Siwy, Z.; Heins, E.; Harrell, C. C.; Kohli, P.; Martin, C. R. *J. Am. Chem. Soc.* **2004**, *126*, 10850–10851.
- (9) Siwy, Z.; Powell, M. R.; Kalman, E.; Astumian, R. D.; Eisenberg, R. S. *Nano Lett* **2006**, *6*, 473–477.
- (10) Minorsky, N. *Nonlinear Oscillations*, Van Nostrand: Princeton, NJ, 1962.
- (11) Diefenderfer, J.; Holton, B. *Principles of Electronic Instrumentation*, 2nd ed.; Saunders College Publ.: Philadelphia, PA, 1994.
- (12) Fleischer, R. L.; Price, P. B.; Walker, R. M. *Nuclear Tracks in Solids. Principles and Applications*; University of California Press: Berkeley, CA, 1975.
- (13) Spohr, R. German Patent DE 2951376 C2, 1983; US Patent 4369370, 1983.
- (14) Wolf, A.; Reber, N.; Apel, P. Y.; Fischer, B. E.; Spohr, R. *Nucl. Instrum. Methods Phys. Res., Sect. B* **2005**, *105*, 291–293.
- (15) (a) Bashford, C. L.; Alder, G. M.; Pasternak, C. A. *Biophys. J.* **2002**, *82*, 2032–2040. (b) Pasternak, C. A.; Bashford, C. L.; Korchev, Y. E.; Rostovtseva, T. K.; Lev, A. A. **1993**, *77*, 119–124.
- (16) Siwy, Z.; Apel, P.; Baur, D.; Dobrev, D.; Korchev, Y. E.; Neumann, R.; Spohr, R.; Trautmann, C.; Voss, K. *Surf. Sci.* **2003**, *532–535*, 1061–1066.
- (17) Savel'ev, S.; Nori, F. *Chaos* **2005**, *15*, 026112/1–026112/16.
- (18) Cervera, J.; Schiedt, B.; Ramirez, P. *Europhys. Lett.* **2005**, *71*, 35–41.
- (19) Nonner, W.; Catacuzzeno, L.; Eisenberg, B. *Biophys. J.* **2000**, *79*, 1976–1992.
- (20) Nonner, W.; Gillespie, D.; Henderson, D.; Eisenberg, B. *J. Phys. Chem. B* **2001**, *105*, 6427–6436.
- (21) Boda, D.; Busath, D.; Eisenberg, B.; Henderson, D.; Nonner, W. *Phys. Chem. Chem. Phys.* **2002**, *4*, 5154–5160.
- (22) Eisenberg, B. *Biophys. Chem.* **2003**, *100*, 507–517.
- (23) Miedema, H.; Meter-Arkema, A.; Wierenga, J.; Tang, J.; Eisenberg, B.; Nonner, W.; Hektor, H.; Gillespie, D.; Meijberg, W. *Biophys. J.* **2004**, *87*, 3137–3147.
- (24) Roth, R.; Gillespie, D. *Phys. Rev. Lett.* **2005**, *95*, 247801 (1–4).
- (25) Brown, T. L.; LeMay, H. E.; Bursten, B. E. *Chemistry. The Central Science*, 8th ed.; Prentice Hall Inc.: Upper Saddle River, NJ, 2000.
- (26) NIST Standard Reference Database 46, <http://www.nist.gov/srd/nist46.htm>
- (27) (a) Hanggi, P.; Bartussek, R. Brownian Rectifiers: How to Convert Brownian Motion into Directed Transport. In *Nonlinear Physics of Complex Systems*; Parisi, J., Mueller, S. C., Zimmermann, W., Eds.; Lecture Notes in Physics 476; Springer: Berlin, 1996; pp 294–308. (b) Astumian, R. D. *Science* **1997**, *276*, 917–922.
- (28) Siwy, Z.; Kosinska, I. D.; Fulinski, A.; Martin, C. R. *Phys. Rev. Lett.* **2005**, *94*, 048102.
- (29) (a) Howard, J. *Mechanics of Motor Proteins and the Cytoskeleton*; Sinauer Associates, Inc.: Sunderland, MA, 2001. (b) Potter, M. J.; Gilson, M. K.; McCammon, J. A. *J. Am. Chem. Soc.* **1994**, *116*, 10298–10299.

NL061114X